NKS-348
ISBN 978-87-7893-431-4

Treatment of ex-vessel debris coolability in IDPSA context

Taneli Silvonen

VTT, Finland

August 2015

Abstract

This study discusses ex-vessel debris bed coolability from safety analysis perspective, espe-cially regarding level 2 probabilistic risk assessment (PRA). The goal is to explore practical and risk-informed ways to deal with debris coolability issues in plant scale risk considerations. Analyses exploit deterministic accident progression simulations which are performed by using MELCOR, and thus this study builds upon IDPSA (integrated deterministic and probabilistic safety assessment) framework.

Literature part covers the most important debris bed parameters that can affect debris coola-bility. Also mechanisms that provide cooling are briefly presented. Empirical research on de-bris coolability has been performed at VTT and also elsewhere, and some results relevant to this study are referred to. Analytical capabilities play a crucial role in coolability assessment and some codes developed for that purpose are introduced in short.

Probability of failure to provide cooling for ex-vessel debris is evaluated by using load vs. ca-pacity concept. Debris bed heat flux is used as load variable and dryout heat flux serves as capacity variable. Two scenarios are employed: pressurized and gravity-driven melt ejection modes. Analyses indicate that when primary system is pressurized when vessel fails, the probability of having non-coolable debris is smaller than in depressurized cases due to e.g. less threatening debris shape and other properties that favour coolability. However, it must be kept in mind that primary system depressurization has other benefits to its name when it comes to severe accident management. All in all, this study provides useful insights to ex-vessel phase of severe reactor accidents with respect to PRA needs.

Key words

Ex-vessel debris coolability, IDPSA, L2 PRA, MELCOR

NKS-348
ISBN 978-87-7893-431-4
Electronic report, August 2015
NKS Secretariat
P.O. Box 49
DK - 4000 Roskilde, Denmark
Phone +45 4677 4041
www.nks.org
e-mail nks@nks.org

Acknowledgements

NKS conveys its gratitude to all organizations and persons who by means of financial support or contributions in kind have made the work presented in this report possible.

Disclaimer

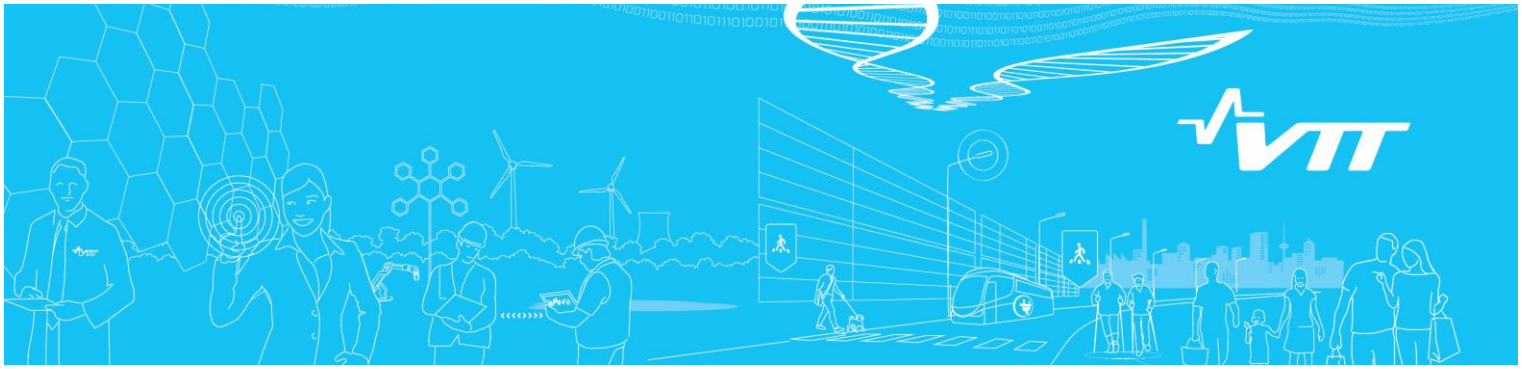

RESEARCH REPORT

VTT-R-02943-14

Treatment of ex-vessel debris coolability in IDPSA context

Author: Taneli Silvonen

Confidentiality: Public

Report's title Treatment of ex-vessel debris coolability in IDPSA context	
Customer, contact person, address State Nuclear Waste Management Fund (VYR)	**Order reference** 7/2011SAF
Project name PRA Development and Application	**Project number/Short name** 85364/PRADA
Author(s) Taneli Silvonen	**Pages** 27/
Keywords Ex-vessel debris coolability, IDPSA, L2 PRA, MELCOR	**Report identification code** VTT-R-02943-14

Summary

This study discusses ex-vessel debris bed coolability from safety analysis perspective, especially regarding level 2 probabilistic risk assessment (PRA). The goal is to explore practical and risk-informed ways to deal with debris coolability issues in plant scale risk considerations. Analyses exploit deterministic accident progression simulations which are performed by using MELCOR, and thus this study builds upon IDPSA (integrated deterministic and probabilistic safety assessment) framework.

Literature part covers the most important debris bed parameters that can affect debris coolability. Also mechanisms that provide cooling are briefly presented. Empirical research on debris coolability has been performed at VTT and also elsewhere, and some results relevant to this study are referred to. Analytical capabilities play a crucial role in coolability assessment and some codes developed for that purpose are introduced in short.

Probability of failure to provide cooling for ex-vessel debris is evaluated by using load vs. capacity concept. Debris bed heat flux is used as load variable and dryout heat flux serves as capacity variable. Two scenarios are employed: pressurized and gravity-driven melt ejection modes. Analyses indicate that when primary system is pressurized when vessel fails, the probability of having non-coolable debris is smaller than in depressurized cases due to e.g. less threatening debris shape and other properties that favour coolability. However, it must be kept in mind that primary system depressurization has other benefits to its name when it comes to severe accident management. All in all, this study provides useful insights to ex-vessel phase of severe reactor accidents with respect to PRA needs.

Confidentiality	Public

Espoo 9.6.2014

Written by	**Reviewed by**	**Accepted by**
Taneli Silvonen Research Scientist	Ilkka Karanta senior scientist	Eila Lehmus head of research area

VTT's contact address
Taneli Silvonen, P.Box 1000, FI-02044 VTT

Distribution (customer and VTT)

SAFIR TR5 & TR8, KTH/P. Kudinov, LRC/Y. Adolfsson, VTT Archive

Preface

This report has been prepared under the research project PRADA, which concerns development and application of probabilistic risk assessment methods. The project is a part of SAFIR2014, which is a national nuclear energy research program. PRADA project work in 2014 is funded by the State Nuclear Waste Management Fund (VYR), Technical Research Centre of Finland (VTT), Aalto University, Nordic Nuclear Safety Research (NKS) and OECD HRP, which is gratefully acknowledged. The work was carried out at VTT.

Espoo, 9.6.2014

Author

Abbreviations

BWR	Boiling Water Reactor
CET	Containment Event Tree
COOLOCE	Core debris coolability and environmental consequence analysis
DHF	Dryout Heat Flux
IDPSA	Integrated Deterministic and Probabilistic Safety Analysis
NPP	Nuclear Power Plant
PRA/PSA	Probabilistic Risk/Safety Assessment
PRADA	PRA Development and Application
RCS	Reactor Coolant System
RPV	Reactor Pressure Vessel

Contents

1. Introduction

In Figure 1.1 are the main phenomena to be considered in management of severe accidents after vessel breach has taken place. Steam and non-condensable gases generation and direct containment heating can induce containment failure due to overpressurization. If melt is ejected into a flooded cavity, steam explosions can occur and expose containment to high instantaneous pressure impulses. Steam explosions have already been considered in PRADA project [1] and the work is planned to go further in 2014. If containment remains intact in melt ejection phase and debris bed forms on the cavity floor, the presence of coolant is a necessary although not sufficient condition for avoiding containment threatening interactions between molten corium and concrete. This work concentrates on debris coolability issue in a flooded cavity, i.e. ex-vessel scenario.

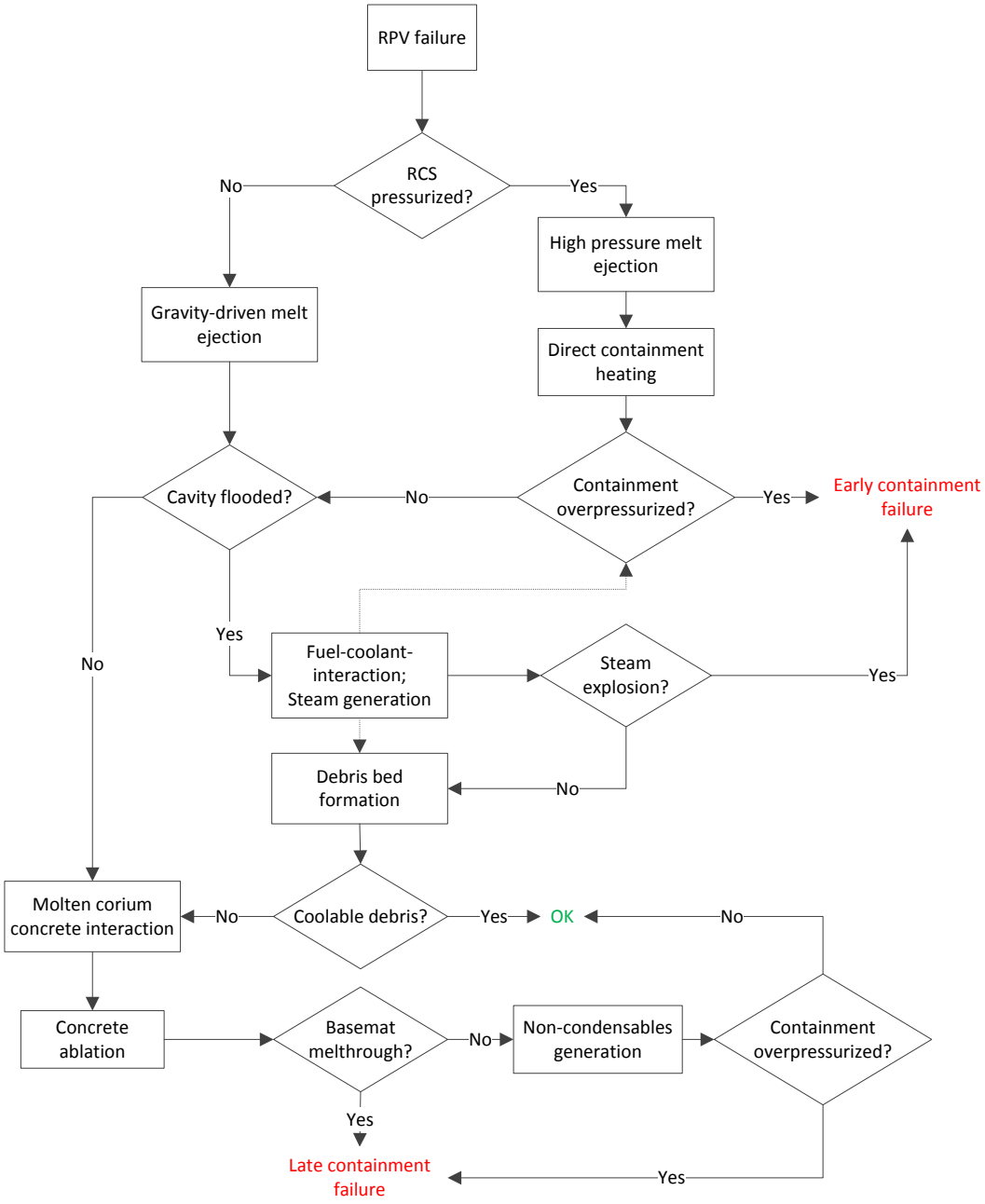

Figure 1.1: Schematic picture of main severe accident phenomena after vessel breach has occurred (modified from [2]).

In Nordic BWRs, the melt from the failed RPV is ejected into a flooded cavity, with water pool depth in the range of 7-11 m. Some plants outside Nordic countries apply different cooling strategies and flood the cavity just after the melt arrival. Phenomenologies of the two methods for melt cooling differ from each other, particularly with respect to melt-water interactions. Newer designs, such as European Pressurized Reactors (EPR) have core catchers where the melt is collected after vessel failure. The common objective of all methods is to reduce interaction between molten corium and concrete and the subsequent basemat penetration or containment over-pressurization. This study concerns the Nordic approach and considers only scenarios relevant to BWR units operated by TVO in Olkiluoto.

Debris coolability is approached here from Level 2 PRA perspective, i.e. uncertainties involved in the issue are taken into account in order to obtain a risk-informed overall picture of the problem and its significance to containment integrity. Integrated deterministic and probabilistic safety analysis (IDPSA) is the methodological framework utilized, i.e. deterministic analyses are combined with probabilistic considerations.

First, phenomenological aspects, including cooling mechanisms and important parameters to coolability, are introduced in section 3. Experimental results and analytical capabilities are also discussed, and synergies with another SAFIR2014 project COOLOCE are exploited. Section 4 deals with IDPSA approach and its application to level 2 PRA purposes. Integral severe accident code MELCOR is used to obtain information on e.g. physical properties of ejected melt. Probabilistic approach to debris coolability modelling is presented, and such an approach could be implemented e.g. in a containment event tree of a level 2 PRA study. The work is a direct continuation to [1] and the same MELCOR model and analysis cases for Olkiluoto nuclear power plant (NPP) units 1&2 are used.

2. Goal

The objective of this work is to enhance ex-vessel debris coolability modelling and understanding in the context of level 2 PRA, i.e. obtain a practical and risk-informed way to deal with coolability issues in plant scale analysis. This is achieved by developing better comprehension of the governing physical phenomena e.g. by exploiting simulations and experimental databases. Special attention is given to treatment of uncertainties. Another goal is to attain methodological progress in IDPSA framework.

3. Ex-vessel debris coolability

If reactor pressure vessel breaches, the core debris (or corium), potentially together with liquid water, steam and non-condensable gases, is released into cavity below the RPV. Preceding accident progression, including core degradation process and accident management measures, affect melt characteristics such as mass and composition. Vessel failure mode, RCS pressure at the moment of vessel breach, water amount and properties in the cavity and cavity geometry all are issues to be taken into consideration in debris coolability assessment. Debris coolability is decisive for containment survival because non-coolable debris eventually leads to containment basemat melt-through or destruction of containment penetrations. In addition, Molten Corium Concrete Interaction (MCCI) produces gases into containment atmosphere and may trigger containment filtered venting or over-pressurize containment.

Debris cooling behaviour is determined for a large part by dryout and quenching. Dryout occurs when heat transfer from water-filled debris is not sufficient to retain debris in such state that no dry zone is formed inside it. Quenching relates to already dry debris and the possibility to flood it and cool down to saturation condition instead of letting it heat up further. Long

term coolability is associated to a steady state where all evaporated water is replaced by water inflow everywhere in the particulate bed. [3]

High-pressure melt ejection effectively means that the melt leaves RPV in jet form, associated with energetic gas discharge. Consequently the melt is fragmented into small particles, and it has a wide spreading area (subject to cavity area constraint). Fragmented corium is more easily coolable than unbroken corium because there is higher total surface area available for heat transfer. Thus large spreading area and high fragmentation increase the possibility to have coolable debris. Also steam explosions can cause melt fine fragmentation. On the other hand, fragmentation can produce a wide distribution of particle sizes which is unfavourable regarding coolability. Gravity-driven melt ejection associated with low RCS pressure results in less dispersed and dense corium collected at the bottom of the flooded cavity, in which case a thick, hard-to-cool particulate debris heap develops.

BWRs have control rod guide tube penetrations through the bottom of the RPV, which may lead to earlier vessel failure due to melt discharge through these penetrations before the steel of the vessel melts. If RPV fails from the bottom penetrations, there will most likely be multiple melt jets, but the melt accumulation in the cavity can still be more gradual compared to direct vessel melt-through due to small break diameters available for melt ejection. RPV bottom penetration failure can also occur relatively early when the meltdown is not complete, effectively meaning smaller melt amounts. Generally speaking, moderate melt pours are favoured over large ones. Similar to other vessel failure modes, the fragmentation of melt ejected through vessel bottom penetrations depends highly on vessel pressure when the failure occurs. Melting of control rod housing and other large structures affects melt composition.

In Nordic BWRs the vessel cavity is filled with water before the arrival of melt, and the pool depth is in the range of 7-11 m [4]. Another approach is to fill the cavity as soon as possible after the arrival of melt. In both cases the water is substantially subcooled. The operative difference between the two methods is in the melt fragmentation process, which affects heat removal from the melt by increasing surface area of the melt. The Nordic approach supports melt fragmentation into small pieces, thus promoting debris coolability, but with the expense of the consequent increase in steam explosion risk. With already flooded cavity it is also more likely that the melt forms a heap-like configuration on the cavity bottom, thus hindering coolability, instead of spreading out more evenly. Of other cooling strategies, promising results have been obtained in experiments where water is added from the bottom of a melt layer. More information of the COMET concept is available e.g. in [5] or [4]. This work focuses on pre-flooded cavity because of its relevance for Olkiluoto NPP units 1 & 2.

Corium and debris coolability issues are actively under research e.g. in SARNET (Severe Accident Research NETwork of Excellence) framework. The project aims to reduce remaining uncertainties and improve physical models in the simulation codes.

3.1 Main parameters affecting coolability

In [6], a thorough introduction to parameters that have influence on debris coolability is given. Coolability itself is often expressed by a physical quantity called dryout heat flux (DHF, unit W/m^2), which means the maximum heat flux that can be removed from the bed through its upper surface. The internal decay power produced in the bed is converted by evaporation of cooling water, and the steam escapes the bed through the upper surface. The maximum steam flux determines the DHF.

When debris is immersed in a pool of water, the produced steam and liquid coolant are in counter-current flow. The steam flux impedes the water flux necessary to replace the evaporated coolant, and when the evaporated liquid can no longer be completely replaced by the inflow, local dryout develops in the debris bed. The main parameters that affect DHF are briefly introduced next. These parameters include bed porosity, particle size, bed height and

system pressure. However, generally it is not possible to determine the coolability of debris by just using bed properties like height and pressure, and more detailed analysis is needed [6]. Also heterogeneities such as differences in local porosities of stratified debris beds complicate the coolability analysis.

Porosity
The porosity of a debris bed volume is defined as the ratio of hollow space and total volume of the bed. For real debris beds (irregular particle size and shape) that might form during severe accident the expected porosity is about 0.4 [6]. For high porosities more cooling liquid is inside the bed, which increases heat transfer. Also friction losses decrease because there is more space available for fluid flow. Thus a higher porosity always corresponds to better coolability.

Particle size
Particle size is connected to the porosity of the bed and smaller particle size also means increased friction for flows. Thus the DHF increases with particle size. The particle diameter effect on DHF is more sensitive for small particles and is not that significant for debris beds consisting of larger particles. Heat transfer process is limited due to small heat conductivity of corium and is affected by particle size as well. However, for realistic particle sizes the heat can be transferred from the particle without remelting in the centre. For multi-grain configurations a mean diameter can be defined to be used in analyses. Experimentally observed particle sizes vary in the range of 1-6 mm [6].

Bed height
In case of fixed power density, the higher the particulate debris bed, the more vapour is generated and has to escape through upper surface of the bed. This means that counter-current flooding limit (where just all evaporated coolant can be replaced) is reached at lower power for deeper beds. However, when debris bed becomes deep enough, DHF becomes independent of the bed height because in the end DHF is given by the total power of the bed, not merely by its height. The limit of deep bed is reached at about 100 times the particle diameter, and for realistic reactor scenarios only deep beds have to be considered due to large corium total mass [6]. More important than bed height is its geometry, inner structure and flow conditions that might enable coolant inflow also from other directions than just the top of the bed.

System pressure
Starting from atmospheric pressure, there is a strong increase in DHF for increasing system pressure, which is explained by increasing steam density: More steam can escape the bed before reaching the counter-current flooding limit. At very high (7 MPa) pressures the latent heat of the evaporation process is decreased which impedes heat transfer and results in decreased DHF. In reactor typical cases, the maximum system pressure is given by the maximum load the containment structure can withstand (around 1 MPa). Thereby in realistic ex-vessel reactor conditions higher system pressure equals better overall coolability.

3.2 Cooling mechanisms

For corium melt layer flooded from top there were four principle mechanisms identified for cooling in the MACE and MCCI projects. Each mechanism is described in [4] and a brief overview of them all is given below.

Bulk cooling
Bulk cooling occurs before a stable crust is formed on the upper surface of the melt layer. When melt attacks concrete, gas is generated at a high rate which leads to enhancement of the interfacial surface area of melt in contact with water. The effective heat transfer coefficient depends e.g. on gas sparging[1] rate, bubble size, thermophysical properties of the mix-

[1] Bubbling of a chemically inert gas through a liquid. [23]

ture, coolant properties and containment pressure. Bulk cooling continues until a stable crust is formed. Stable crust forms when melt temperature decreases to melt solidus temperature and gas sparging rate drops so that formation of a stable crust is possible.

Water ingression
Once a stable crust has formed the liquid melt is isolated from water and the only heat transfer process is through the crust, which is an ineffective way of removing heat. However, there are cracks and porosities in the crust formed by escaping gases which provide pathways for water to ingress into the crust. Water ingression also leads to development of additional cracks due to quenching of the crust. Water ingression can be understood as a process that thins the thermal boundary between crust and melt and thus enhances heat transfer. Water ingression is highly dependent on the crack propagation process.

Melt eruption
Because cracks present in the crust cannot vent all the gases produced by core-concrete interactions, it is possible that pressure under the crust accumulates locally so that a volcano-like eruption of liquid melt occurs through the crust surface. Erupted melt gets in contact with water above the crust surface and fragments into a particle bed, which is then cooled by the overlaying water. Therefore melt eruptions are effective events to transfer heat underneath the crust surface to the water pool above the crust. Melt eruptions generally occur when heat removal rate from the liquid melt falls below decay heat generation rate. Thus melt temperature increases, concrete erosion becomes more rapid and more gases are generated. Increased gas generation cannot be accommodated by the flow through the crust and an eruption takes place. Melt entrainment coefficient is of great significance for evaluation of heat transfer through melt eruption.

Crust breach
When crust is suspended and spans over the whole lower drywell/cavity of the containment (attached to the sidewalls), it is practically a certainty that water masses above the crust induce a crust breach. Once crust has breached, water gets in contact with liquid melt again and a new debris cooling cycle begins, i.e. the processes of bulk cooling, crust formation, water ingression and melt eruption. Repetition of this cycle enables extraction of great amounts of heat from the liquid melt and can eventually lead to solidification of all liquid melt. Analyses indicate that over one third of the melt needs to be in crust form so that the crust would be stable in a 6 meter diameter cavity [4]. In case of crust floating over a liquid melt pool without being attached to the walls, crust breach is out of question. According to [4], the most probable configuration would involve crust attached to the cavity walls with a floating crust area in the middle. However, no crust breach has thus far been observed in any melt coolability experiments that have been performed.

3.3 Experimental research

There have been many research projects, some of them in Finland, where experiments on different phenomena relevant for debris coolability assessment have been conducted. A good overview is given in [4], and merely a list of some projects and their objectives is given here. The objective of most investigations has been to determine the dryout heat flux discussed in section 3.1 [3].

MACE program run by Argonne Natural Laboratory (ANL) in late 1980s aimed to demonstrate coolability of core melt pools by using large scale test facilities. MACE experiences helped to identify the cooling mechanisms discussed in section 3.2. MACE project was followed by the MCCI-1 and MCCI-2 projects, but these projects could not confirm debris coolability with top flooding although they increased analytical capabilities and understanding of the topic. Results from these experiments have been used in development of CORQUENCH code. DEBRIS experiments performed at Istitut für Kernenergetik und Ener-

giesysteme (IKE) focused on constitutive laws, such as friction and heat transfer, under boil-off and quenching conditions.

FARO experiments investigated the breakup of melt jet penetrating into water pool. An important outcome was the observation that realistic reactor conditions yielded significant melt breakup. Also variations in conditions were observed not to have any significant influence on particle size distributions. FARO experiments are considered most relevant fuel breakup experiments using prototypic corium material, thick jets, large masses and long pours [4]. KROTOS experiments also concentrated on melt breakup, although smaller melt amounts were used than in FARO, and results showed smaller particle mean sizes. DEFOR experiments at KTH (Royal Institute of Technology) investigated debris bed formation from breakup of melt and results indicated for example higher porosities in the debris bed than previously assumed.

The STYX experiments [7] performed at VTT concerned mixed particle shapes and size distribution from FARO experiments to assess prototypic debris behaviour. Irregular gravel was used as simulant material. Uniformly spread 60 cm high electrically heated debris bed, cooled by top flooding, was used. The goal of the project was to qualify the use of a deep ex-vessel water pool as a severe accident management measure. Experimental DHF results were quite low, partly because of small effective particle diameter. At atmospheric pressure, the measured DHF value was only 232 kW/m^2, and in 0.7 MPa pressure DHF increased to 451 kW/m^2. The study concluded that at low pressures debris coolability could be a problem at Olkiluoto plant. STYX experiments may be considered more as yielding results for basic investigations and code validation than directly usable for reactor scenarios [8].

Table 3.1: Some results from dryout heat flux measurements with top flooding conditions. H=Homogeneous bed, S=Stratified bed. Reproduced from [7].

Test	Pressure [MPa]	Particle diameter [mm]	Porosity	Bed depth [m]	DHF [kW/m^2]
Purdue (H) [9]	0.1-0.24	8	0.386	1.016	821-1100
Winfrith (H) [10]	0.1-0.9	0.2-5	-	0.05-0.15	960-1350
DCC-1 (H)	0.1-17.0	0.71	0.345	0.5	40-80
DCC-2 (H) [11]	0.1-17.0	2.43	0.41	0.5	500-1100
KfK (H) [12]	0.1	0.2-0.5	0.395	0.2	58-60
SILFIDE (H) [13]	0.1	2 3.4 4.7 7.1	0.4	0.5	700 1000 1500 1650
POMECO (H) [14]	0.1	0.2 0.9	0.4	0.45	90 222
DCC-3 (S) [15]	0.07-6.9	4.67+1.18	0.41	0.5	117-285
POMECO (S) [16]	0.1	0.9+0.2	2.36-0.36	0.37	54-122

Ref. [7] also lists results from earlier experiments on debris bed dryout heat flux, and Table 3.1 is reproduced from [7]. Most of the data in Table 3.1 concerns single-sized, spherical

particles, but some data exists also for irregularly shaped multi-grain configurations. Generally speaking, the data is highly scattered and it is difficult to draw any explicit conclusions.

3.3.1 COOLOCE experiments

There is active research on coolability issues at VTT, and the STYX experimental facility has been followed by COOLOCE test facility. First experiments covered top-flooded cylindrical debris bed and a conical, heap-like bed. Later the test programme has been extended to include e.g. a cylindrical bed with lateral flooding. The objective is to find out the coolability limits in well-defined representative conditions. Table 3.2 shows different test configurations that have been implemented.

Table 3.2: Summary of the COOLOCE experiments. [17]

Experiment	Test bed	Flow configuration	Particle material	Pressure range [bar]
COOLOCE-1-2	Conical	Multi-dimensional	Spherical beads	1.6-2.0
COOLOCE-3-5	Cylindrical	Top-flooding	Spherical beads	1.0-7.0
COOLOCE-6-7	Conical	Multi-dimensional	Spherical beads	1.0-3.0
COOLOCE-8	Cylindrical	Top-flooding	Irregular gravel	1.0-7.0
COOLOCE-9	Cylindrical	Top-flooding	Irregular gravel	1.0
COOLOCE-10	Cylindrical	Top-flooding & lateral	Spherical beads	1.3-3.0

The COOLOCE facility consists of pressure vessel containing particle bed section, heating equipment and feed water and steam removal systems. Conical and cylindrical test beds are 500 and 310 mm in diameter, respectively. Electrical resistance heaters simulate the decay heat, and aim is to achieve volumetrically uniform power distribution. Geometry comparison experiments were performed with spherical beads, whereas particle material effects were studied with irregularly shaped and sized gravel particles.

COOLOCE tests have clarified that the coolability of conical debris bed is reduced around 50% compared to cylindrical bed of equal volume because of greater height of conical beds. If debris beds are of equal height, the tests suggest that conical bed is better by 50-60% in terms of coolability provided by lateral flooding.

The dryout heat flux measured for alumina gravel was low compared to the experiments with spherical beads, and also slightly lower compared to experiments with the STYX facility. The difference is explained by the greater average size of the beads, which increases coolability. For gravel beds, the important parameters (particle diameter, porosity) to which dryout heat flux is sensitive are not as well-known as for spherical beds [17].

Test configurations have also been analysed using 2D MEWA simulations [18]. The agreement between results and experiments varies between very good and reasonable. For instance it seems that simulations tend to underestimate coolability of conical beds. MEWA simulations have been complemented by 3D calculations with in-house code PORFLO and FLUENT, but these modelling capabilities are not yet ready for systematic prediction of dryout power [17].

As an example, some experimental DHF results and corresponding simulation results are shown in Table 3.3 for comparison. There were several simulation cases with slightly varied input parameters for each experiment configuration, but results from just one simulation for each experiment is shown in Table 3.3. Both experimental and simulation results seem quite low in comparison to values in Table 3.1 but are of same order of magnitude with the STYX experiment.

Table 3.3: Comparison of experimental and simulation results for dryout heat flux. Heat flux unit is kW/m^2. [18]

Pressure [bar]	COOLOCE-3-5		COOLOCE-8	
	Experimental	Simulated	Experimental	Simulated
1.1	270	219	178	171
2.0	347	331	235	240
3.0	422	384	263	287
4.0	458	437	290	328
5.0	493	484	319	356
7.0	560	556	342	411

3.4 Modelling capabilities

Classical coolability analyses have mainly considered 1D homogeneous debris beds (uniform height) under top flooding. The bed is assumed initially to be filled with water and to be in a quenched state, which in practice is not true even with deep water pools. If sufficient water supply can be established to replace evaporated water and to remove decay heat from the bed, no dry zones develop. Classical 1D approach underestimates coolability [4].

More realistic configurations, that is, heap-like heterogeneous debris beds with multidimensional flows, can be analysed by using validated 2D/3D computer codes. Multiphase flow of steam and surrounding water upwards and melt particles downwards requires special attention, as well as laws of friction and debris quenching. Modelling of friction forces is decisive [3] because they determine how much water can enter the debris bed and how fast the produced steam can be removed. Well known classical friction models include Lipinski's model and two phase friction models are generally based on Ergun's law [3]. Level of detail in terms of physical mechanisms in such codes makes them applicable for large spectrum of reactor scenarios.

Some examples of codes used to analyse debris coolability and also other phenomena that affect coolability are given next. The CORQUENCH code developed by ANL utilizes data obtained from MACE project (see section 3.3) and its successors. It has models describing different cooling mechanisms and it can perform analysis for coolability of a corium melt pool interacting with concrete. IKEJET/IKEMIX is a combined jet breakup and settling code developed at IKE of University of Stuttgart. MC3D code from CEA and IRSN in France can be used for similar purposes. IKE also has WABE module for cooling analysis and MEWA module for combined melting and cooling analysis included in ATHLET-CD, which is used to assess accidents resulting from major core damage. Data obtained from experiments has been vital for validation of constitutive laws in codes mentioned above. Also integral accident

analysis codes are useful because they can help to determine the initial conditions, such as melt amount and composition for the debris to be cooled, as well as e.g. ambient pressure.

4. Risk-informed treatment of debris coolability

Coolability of debris/corium depends on many things, as discussed in section 3. The situation is highly case and reactor-specific and as realistic consideration as possible is important. As stated in [19], ex-vessel debris coolability is subject to large uncertainties and any "over-simplified" conclusion on this topic should be avoided. However, some reasonable simplifications are needed for level 2 analysis so that the issue could be included in containment event trees without giving it merely a probability value.

In [20], debris bed dryout probability is estimated by using the concept of load vs. capacity. The analyses use Monte Carlo simulations and distribution functions for parameters that affect heat fluxes, thermal power or melt mass which all can be used to define load and capacity variables. A surrogate model that gives dryout heat flux is developed for cone shaped debris bed by generalizing two dimensional dryout simulations. It is also highlighted that load and capacity variables (e.g. heat flux and dryout heat flux, respectively) are often interconnected through accident scenario and severe accident management measures taken.

Several debris bed geometries are considered in [20], including flat and conical shapes as well as a cone that stands on a cylindrical base. A purely conical debris bed with mass M, density ρ and porosity ε has volume $V = M/\rho(1-\varepsilon)$, and the height of such bed can be written as

$$h = \left(\frac{3M\tan^2\alpha}{\pi\rho(1-\varepsilon)}\right)^{\frac{1}{3}}, \tag{1}$$

where α is the slope angle. Heat flux HF produced by a flat debris bed of height h and specific decay heat power W can be expressed as

$$\mathrm{HF} = \rho(1-\varepsilon)Wh. \tag{2}$$

This expression for heat flux can be used also for conical debris beds by considering the location most prone to dryout, i.e. the centre of the bed which corresponds to the top of the heap. From numerical simulations and by considering an infinitely thin vertical cylinder passing through the top of the debris bed it can be assumed that most vapour escaping from the cylinder exits from top of it, i.e. non-vertical flows can practically be neglected. However, coolability of such debris configuration is better than that of a flat debris due to water penetrating the side walls. Thus for a conical debris HF stands for local heat flux instead of an average value and h is the maximum height of the debris heap. By using equations (1) and (2), the expression for heat flux at the top of a debris cone becomes

$$\mathrm{HF} = \left(\frac{3M(1-\varepsilon)^2\rho^2\tan^2\alpha}{\pi}\right)^{\frac{1}{3}} W. \tag{3}$$

Specific decay heat power W is a function of melt release time t_{mr} which is measured as time elapsed since reactor scram. Also nominal thermal power Q_0, total corium mass M_0 and relative power p_r are present in the expression for specific heat power:

$$W(t_{mr}) = \frac{Q_0}{M_0} \cdot \frac{p_r(t_{mr})}{100\%}. \tag{4}$$

Relative power p_r at the time elapsed since reactor scram t_{el} is defined with respect to nominal power and ANS 5.1 standard tables provide values for it. In [21], an approximation of the ANS curve is given as

$$p(t_{el}) = 5 \cdot 10^{-3} a\left[t_{el}^{-b} - (t_s + t_{el})^{-b}\right], \quad (5)$$

where t_s is time of reactor scram measured from the time of reactor start-up (i.e. $t_s + t_{el}$ is the total time since reactor start-up). Parameters a and b depend on t_{el} as follows:

Time after shutdown [s]	a	b
0-10	12.05	0.0639
10-150	15.31	0.1807
150-8E8	27.43	0.2962

Recall that dryout heat flux (DHF) is defined as the maximum local HF so that no dryout occurs. Similar to HF, also DHF in this formulation is attributed only to the top point of a non-flat debris configuration. Surrogate models for dryout heat flux have been developed in [20] and [22], and the idea of these models is to extend DHF concept of a flat debris bed to multidimensional cases. For example in [20] the improvement of coolability of a cone-shaped debris bed due to water inflow from the sides is taken into account by writing DHF as a product of dryout heat flux for a flat bed DHF_{flat} and function Φ that accommodates the shape effects:

$$\mathrm{DHF}\left(d, \varepsilon, P_{sys}, \alpha\right) = \mathrm{DHF}_{flat}\left(d, \varepsilon, P_{sys}\right) \cdot \Phi(\alpha). \quad (6)$$

DHF_f for a particular parameter set is obtained by solving one dimensional problem and Φ is then approximated with help of two-dimensional DHF simulation results. Once this surrogate model has been given its functional form there is no need for further time consuming two-dimensional DHF simulations. Note that function Φ that describes debris shape is here a function of only α but could be more complicated as well.

Reference [23] builds on the approach discussed above and aims at quantification of associated uncertainties by investigating different parameter ranges and distribution shapes. It was observed that uncertainties regarding particle size and the slope angle of the debris heap appear most significant uncertainty contributors. It is also highlighted that correlations between individual parameters should be taken a closer look at.

4.1 IDPSA approach

In this section the risk-informed approach to debris coolability issue discussed above is utilized together with results obtained from MELCOR simulations that were performed earlier and reported in [1]. Thus the analyses are performed within the IDPSA methodological framework. Those accident scenarios analysed in [1] that resulted in vessel melt-through are revisited from ex-vessel debris perspective. Thereafter distributions for both heat flux and dryout heat flux are determined by using Monte Carlo simulation in order to obtain a probability estimate for debris coolability. In the end, an approach to deal with ex-vessel debris coolability in L2 PRA context is suggested for two scenarios, namely high and low pressure accident sequences.

4.1.1 MELCOR simulations

Six different cases were studied with MELCOR in [1], and they can be seen in Table 4.1. The table contains time points for e.g. when the fuel cladding temperature exceeds oxidation threshold for zirconium (1100 K) and when the core melt relocation starts. Only cases 2, 5 and 6 end up with melt ejection into LDW, and are therefore interesting for ex-vessel debris coolability considerations. Other cases are not paid further attention here and the corresponding columns in Table 4.1 are faded.

Table 4.1 provides quite general information about the cases analysed and the most relevant quantities for debris coolability analyses are the system pressure and the amount of melt ejected. As discussed in section 3.1, high ambient pressure results in higher steam density and thus improves coolability through increased dryout heat flux. In that sense, case 6 appears most favourable to debris coolability. However, case 6 also results in biggest melt amounts, which hinders coolability, and pressurized melt ejections are generally less predictable than their gravity-driven counterparts.

Table 4.1: The analysis scenarios studied in [1]. Cases 2, 5 and 6 resulted in melt ejection into LDW and are taken into further consideration here.

	Case #					
	1	2	3	4	5	6
ECCS availability?	Recovery at 3000s	Recovery at 4000s	Recovery at 18000s	Recovery at 19000s	No	No
Depressurization through ADS [s]	1821	1821	-	-	1805	-
Core dry for the first time [s]	2510	2510	4650	4650	2510	4650
Zr oxidation starts [s]	2620	2620	3080	3080	2620	3080
Core support structures start to fail [s]	-	5678	7534	7534	5093	7534
Vessel breach (VB) [s]	-	17447	-	19021	13706	19018
Filtered venting (system 362) [s]	-	-	-	19078	-	19087
LDW water subcooling at VB [K]	-	65.53	-	95.84	73.61	95.84
LDW water partial pressure at VB [bar]	-	1.82	-	3.72	2.25	3.72
Melt ejected [ton]	-	159.7	-	-	183.3	185.5

Some further MELCOR analyses for the three cases were conducted and graphs from Figure 4.1 to Figure 4.5 illustrate some results relevant to ex-vessel debris considerations. Horizontal axes begin from the time of vessel failure which varies from case to case as can be seen from Table 4.1. For each case the last observation is from time 36000 s, i.e. ten hours have been simulated in total.

Heat flux was estimated as the ratio of heat loss from debris surface to debris pool upper surface area, and the results are in Figure 4.1. It appears that case 5 yields the highest initial heat flux over 2 MW/m^2. Also case 6 reaches heat flux values over 1 MW/m^2, and case two seems most favourable to cooling, probably because emergency core cooling has been initiated at the time 4000 s. In both cases 5 and 6 ECCS is unavailable but the difference is that case 5 is depressurized and the melt heats up faster. After oscillating behaviour right after vessel breach all the cases settle at around 0.20 MW/m^2.

Figure 4.2 shows at which power heat is transferred from debris bed to concrete underneath it. Also this time case 5 seems the most challenging and case 2 a little less severe. The meaning of such a variable in MELCOR is to illustrate how much heat goes to ablation of concrete. Figure 4.3 shows the thickness of debris bed for each case and it correlates almost completely with the ejected melt amounts because MELCOR assumes melt to spread evenly in the reactor cavity/LDW. Thus case 6 results in deepest bed. Debris is assumed to consist of 5 layers in MELCOR, namely heavy and light oxide layers, metallic layer and heavy and light mixture layers. In the simulations performed in [1] the debris bed consisted entirely of the heavy mixture layer.

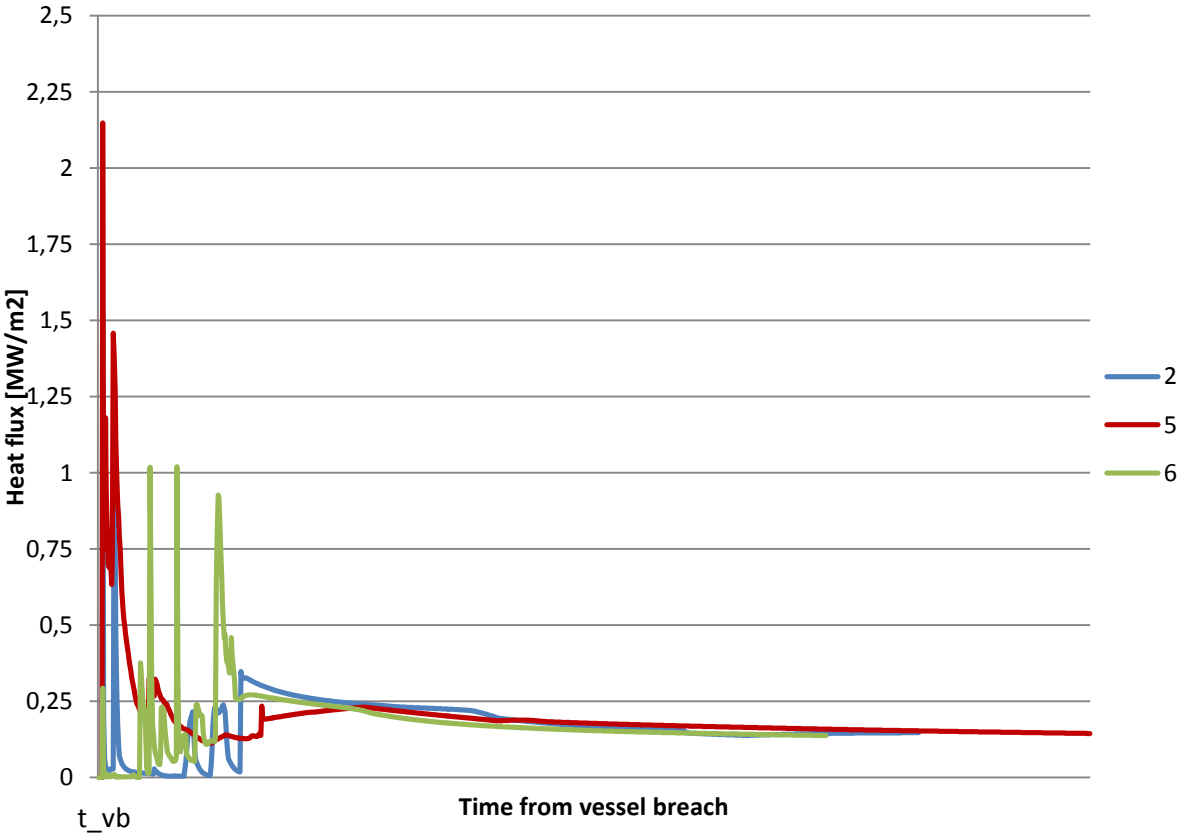

Figure 4.1: Heat flux through the top surface of the debris bed.

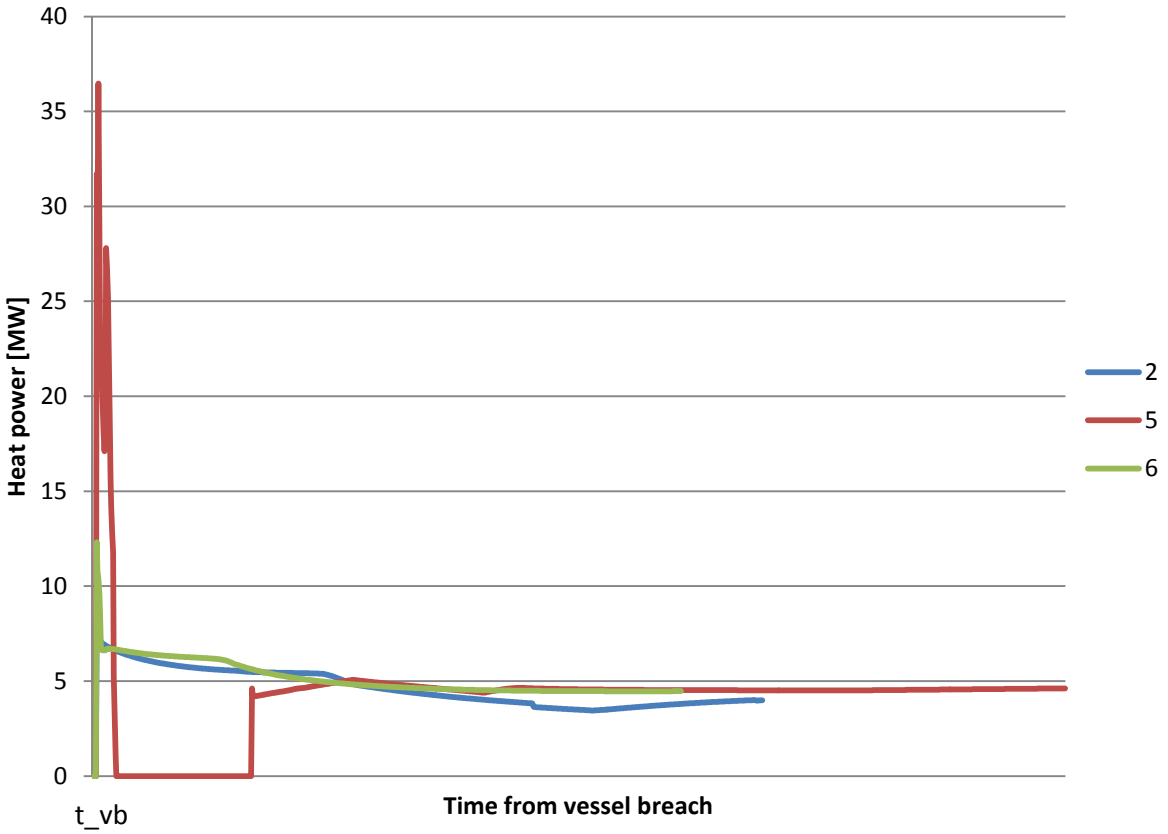

Figure 4.2: Heat loss from debris bed to concrete. Heat goes to ablation of concrete.

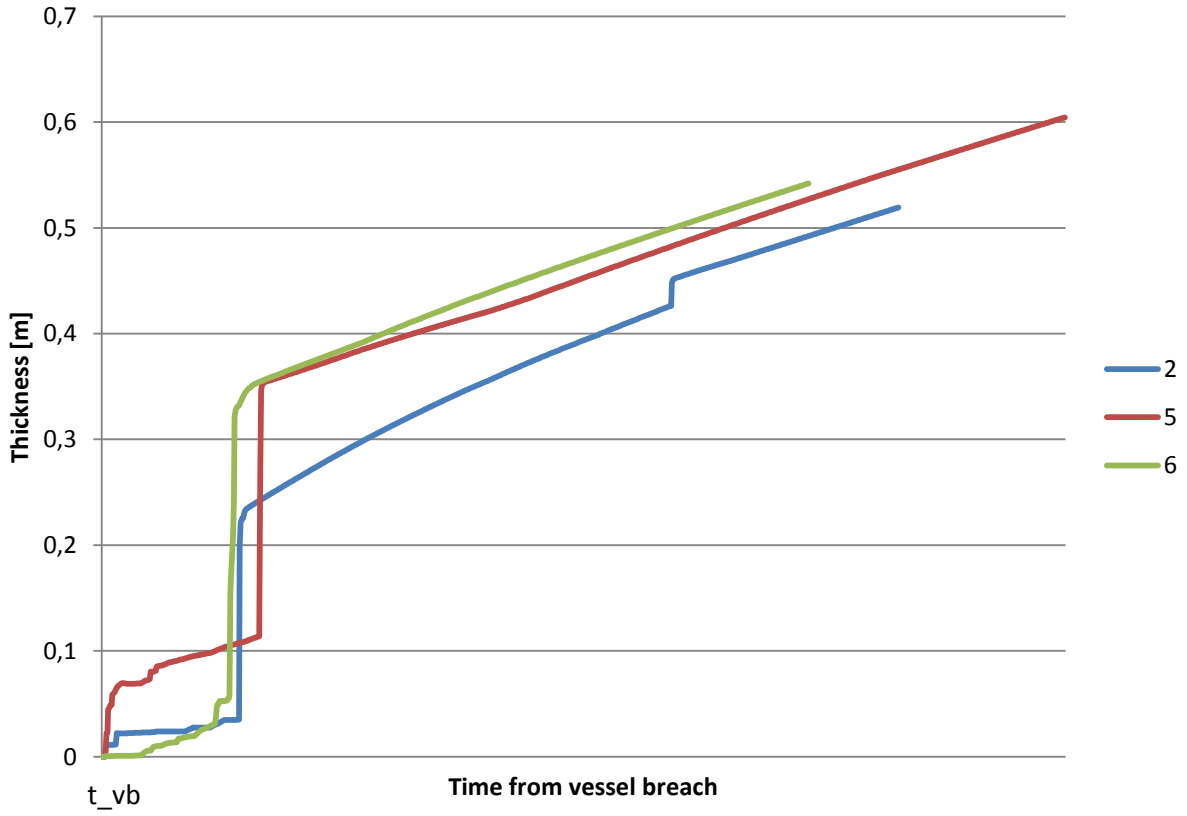

Figure 4.3: Thickness (of the heavy mixture layer) of the debris bed.

In Figure 4.4 are temperatures of the debris beds formed in the analysis cases. Right after vessel breach there is a temperature peak in case 5 and a smaller one in case 2 but they even out quite soon. Only somewhat after vessel failure debris temperatures start to rise rapidly and reach values little less than 2000 degrees centigrade. Delay in temperature rise is due to gradual growth of the vessel breach size which initially permits only small melt amounts to eject. Eventually case 6 yields highest debris temperatures and case 2 has debris temperatures notably lower because the melt was cooled already within the RPV.

Figure 4.5 shows densities of debris beds. Density maxima are attained right after all the melt is released from the vessel and case 2 seems to produce the densest corium with density over 8000 kg/m^3. After maxima have been reached the densities start to decrease in an exponential manner because corium composition changes when concrete is ablated.

Table 4.2 collects the above discussed debris information from MELCOR simulations. Altogether it seems that case 5 with successful depressurization and without ECCS is most severe in terms of heat fluxes. Case 5 results also in thickest debris bed because of earlier vessel failure which enables longer time available for concrete ablation. Case 2 appears least threatening, thanks to ECCS which starts to provide additional cooling at the time 4000 s. With respect to safety analysis, it is interesting to see the effect of depressurization on debris bed properties. By comparing cases 5 and 6, depressurized case seems more severe regarding heat fluxes. At the same time it must be kept in mind that high pressure melt ejection was not implemented in MELCOR model. Thus the effect of different debris bed shape and internal structure caused by pressurized melt ejection is not included in the results.

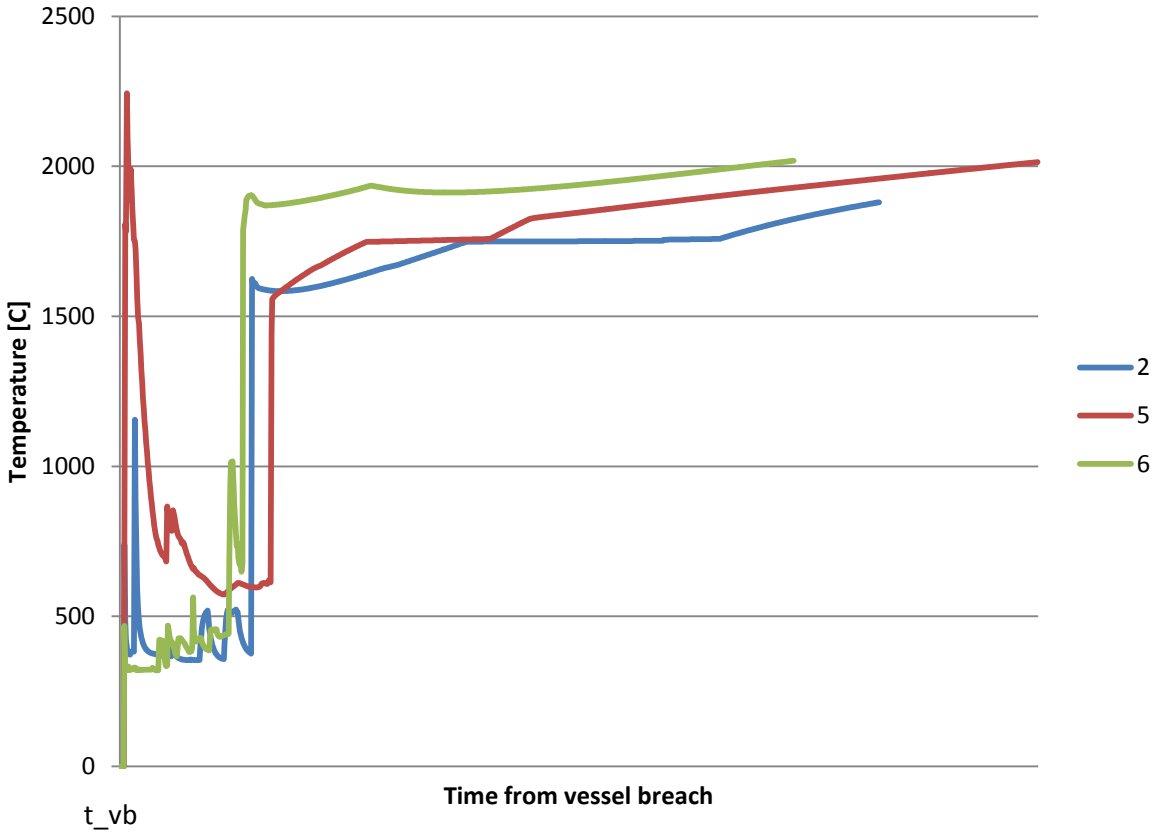

Figure 4.4: Temperature (of the heavy mixture layer) of the debris bed.

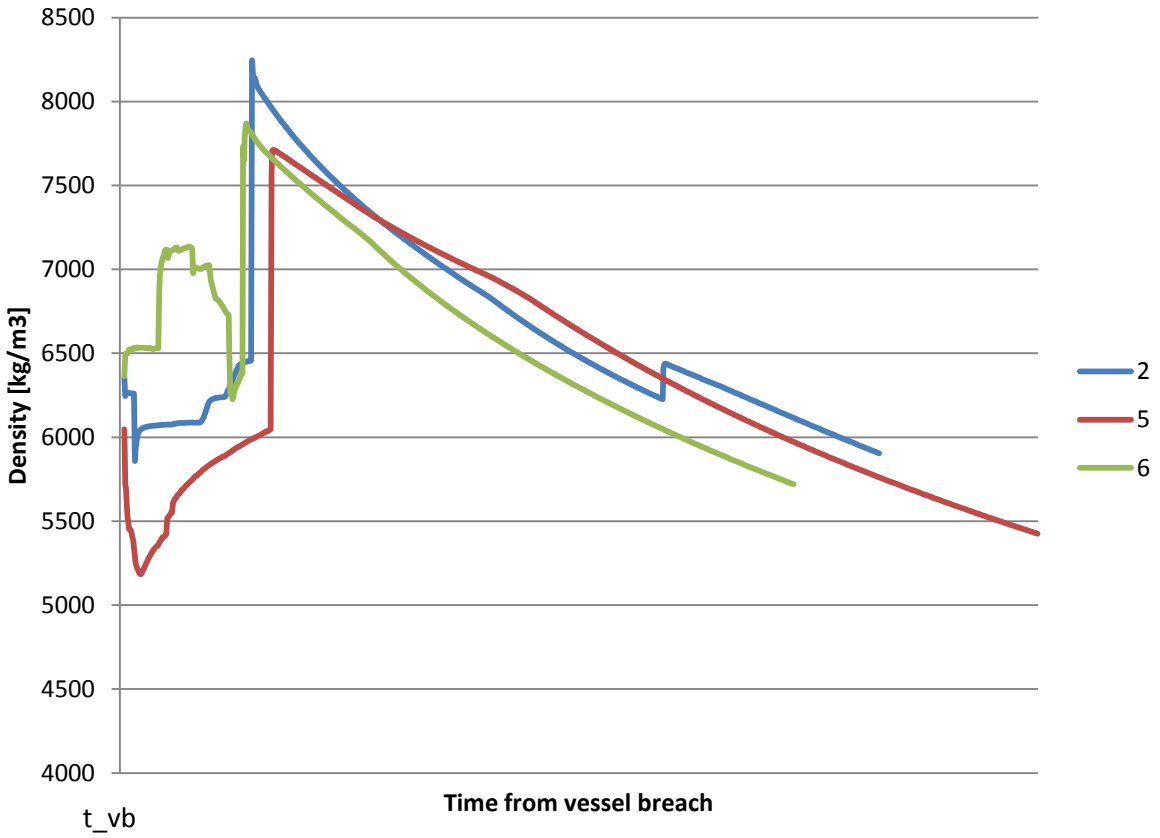

Figure 4.5: Density (of the heavy mixture layer) of the debris bed.

Table 4.2: Case specific debris properties obtained from MELCOR simulations.

	Case #		
	2	5	6
Maximum heat flux [MW/m^2]	1.518	2.148	1.020
Average heat flux [MW/m^2]	0.171	0.194	0.177
Average heat power to concrete [MW]	4.64	4.23	5.11
Bed final thickness (flat) [m]	0.52	0.60	0.54
Final temperature [°C]	1879	2013	2018
Maximum density [kg/m^3]	8245	7712	7869

The plots and results discussed above are provided by MELCOR's CAV package, and there are several details (introduced in [24] and [25]) worth knowing about debris bed modelling used in MELCOR. In CAV package, it is assumed that water cannot break up or penetrate debris and heat can only be removed from debris by conduction to the surface. Thus formation of a coolable debris bed is not feasible. However, quenching can be promoted by modifying parameters that affect thermal conductivity. Concrete ablation affects debris composition so that molten concrete oxides and molten steel from reinforcing bars in concrete are added to the debris pool. By default, debris formation is treated by enforcing complete mixing where debris consists of a single layer, which is spread uniformly and instantaneously across the cavity.

CAV package concentrates on corium attack on basemat concrete and lacks explicit models for quenching and dryout of ex-vessel debris. However, such models are available for in-vessel phase through the COR package. Heat transfer from debris bed to the overlying pool of water following debris bed dryout is assumed relatively modest. Dryout heat flux is calculated with Lipinski 0-dimensional correlation, and it is then applied as a limiting maximum heat transfer rate from debris bed. 0-dimensional Lipinski model has been developed for uniform and homogenous beds and provides reasonable enough estimates for dryout heat fluxes in most reactor application cases [26].

4.1.2 Probabilistic implementation

The probability of having non-coolable debris is evaluated for high and low pressure scenarios using the risk-informed IDPSA approach that has been discussed in the preceding sections. The actual probability is calculated from load vs capacity (or stress vs. strength) concept, where heat flux represents load and dryout heat flux is interpreted as capacity. Heat flux is estimated by using equations (3)-(5) and Monte Carlo method, i.e. parameter values used to calculate heat flux are sampled from probability distributions assigned to them. After n heat flux values have been sampled, a normal distribution is fitted into data. Distribution for dryout heat flux is obtained principally from experimental results discussed in section 3.3, but uncertainty is incorporated by formulating normal probability distribution for DHF.

In Table 4.3 are the parameter values that are used to sample a distribution for heat flux. Nominal thermal power Q is common for both low and high pressure cases and the value represents a typical Nordic BWR. Also total corium mass and corium density are independent of the case in question. Corium density has been given a value 7660 kg/m^3 in [27], and it can be regarded as a typical value for a Nordic BWR. According to MELCOR simulations a uniformly distributed density value between 7500-8000 kg/m^3 is used in this study. It is assumed that the melt amount ejected is bigger for high pressure case because of additional

forces pushing the melt out. Also MELCOR analyses indicate that high pressure cases may involve higher proportion of fuel in a molten state when the vessel fails. High pressure cases support finer fragmentation of melt which affects particle size and thus also debris bed porosity. Therefore porosity is given a smaller value when melt is released at high pressure. Another feature of high pressure scenarios is the spreading of the melt. When melt is released with high velocity it is expected to spread more evenly around the LDW and formation of heap-like debris configurations is less likely than in low pressure cases. Thus slope angle and its range is smaller for high pressure cases than for their low pressure counterparts. Note that nonetheless in both cases a completely flat ($\alpha = 0°$) bed is considered feasible. Time elapsed since reactor start-up is assumed to have a mean value of a year in both cases, with upper limit of two years. According to MELCOR results it seems that in pressurized scenarios it takes a longer time (measured from reactor scram) for vessel to fail than in low pressure cases.

Table 4.3: Parameter values used to estimate heat flux for low and high pressure cases. When a parameter is given a range of values, uniform distribution is assumed.

Parameter	Depressurized case	Pressurized case
Nominal thermal power Q [MW]	2500	2500
Corium density ρ [kg/m^3]	7500-8000	7500-8000
Total corium mass M_0 [tons]	200	200
Corium mass ejected M [tons]	100-200	150-200
Porosity ε	0.3-0.4	0.2-0.3
Bed slope angle α [degree]	0-25	0-15
Time since reactor start-up [years]	0-2	0-2
Time of melt release since reactor scram [s]	10000-20000	15000-25000

Distributions for dryout heat fluxes that represent the capacity variable in the load vs. capacity concept are derived principally from experimental results shown in Table 3.1 and obtained in COOLOCE experiments. Dryout heat flux distribution mean is given quite high values, partly because also the approach used to determine heat flux yields somewhat bigger values than maybe expected beforehand.

It is not straightforward to assess the difference of pressurized or depressurized melt release on coolability of debris bed. For high pressure scenarios the bed is less porous due to finer fragmentation and smaller particles, which has a decreasing effect on dryout heat flux. On the other hand the melt is spread more evenly and it is less likely that pileup of corium leads to extreme local vapour generation which would impede coolant flow into the bed, thus lowering DHF. Pressurized melt ejection, according to MELCOR simulations, is associated with elevated ambient pressure which makes escaping steam denser and eases its way out of the bed, and therefore it has an increasing effect on DHF.

Although there are rivalling mechanisms affecting dryout heat flux, it is assumed in this study that pressurized melt ejection results in slightly elevated DHF values in comparison to low pressure scenarios. To verify this assumption, investigation of combined effect of parameter variations would be useful but it would necessitate a design of experiments type of approach which is not possible at the time. Therefore one has to be content with the reasoning above.

Table 4.4 contains the normal distribution parameters for both heat flux and dryout heat flux in both low and high pressure cases. Parameter values for heat fluxes are obtained by fitting a normal distribution into heat flux data generated with a 10000 samples, whereas DHF distributions are determined by using own judgment and experimental data. DHF distribution for

pressurized case is obtained from depressurized case by a linear transformation of normally distributed random variable X by assuming a 5% increase, i.e. $Y = a + b \cdot X$, with $a = 0$ and $b = 1.05$. Figure 4.6 and Figure 4.7 show the load and capacity distributions for low and high pressure cases, respectively. Already from these figures it is easy to see that probability of having a non-coolable debris bed is, according to this analysis, significantly higher when primary system depressurization has failed than for high pressure cases.

Table 4.4: Normal distribution parameter values for heat flux and DHF in both low and high pressure scenarios.

	Normal distribution parameters	Depressurized case	Pressurized case
Heat flux	Mean μ [kW/m^2]	475.0	350.3
	Std. deviation σ [kW/m^2]	221.6	157.3
Dryout heat flux	Mean μ [kW/m^2]	800.0	840.0
	Std. deviation σ [kW/m^2]	100.0	105.0

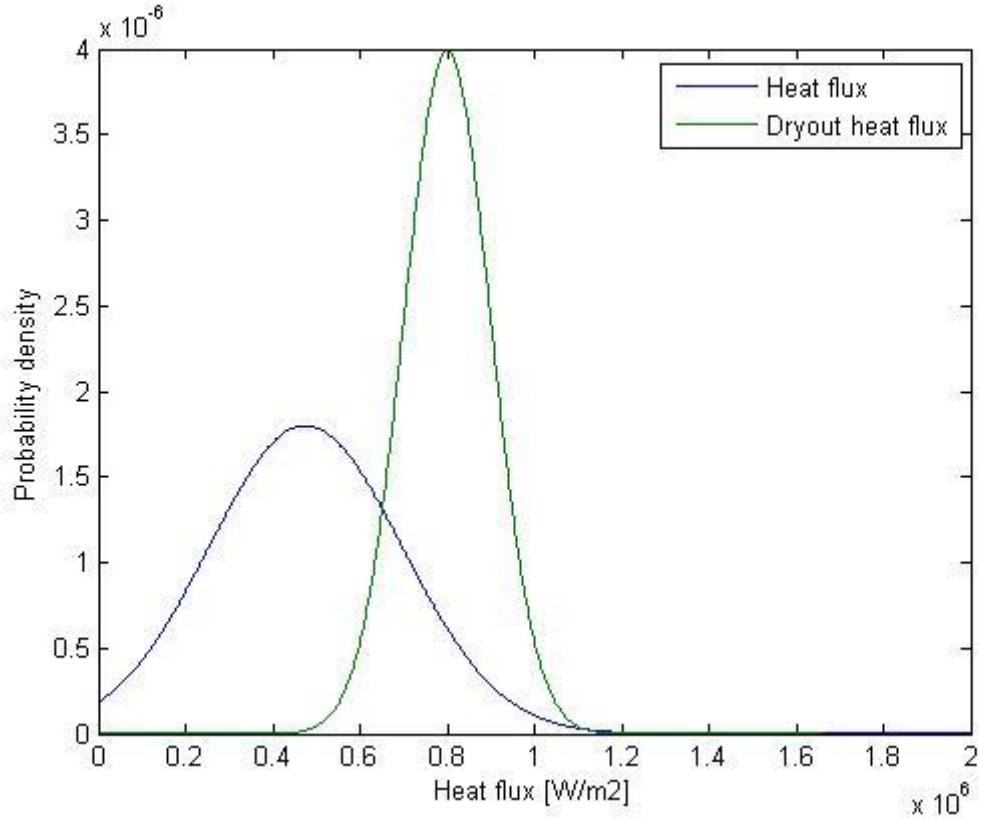

Figure 4.6: Probability density functions for heat flux and dryout heat flux in low pressure case.

With explicitly defined probability distributions it is possible to calculate exact probabilities of having a non-coolable debris bed (i.e. probability of load exceeding capacity) by using expression

$$\mathrm{P(L > C)} = \int_0^\infty f_C(c) \left[\int_c^\infty f_L(l)\mathrm{d}l \right] \mathrm{dc}, \qquad (7)$$

where f_C and f_L are the probability densities for capacity and load variables, respectively. The probabilities were calculated using Mathematica and are shown in Table 4.5, and the

difference is quite significant in favor of pressurized melt ejection scenario. Depressurized cases result in non-coolable debris with 9% probability whereas in pressurized cases have only 0.5% probability.

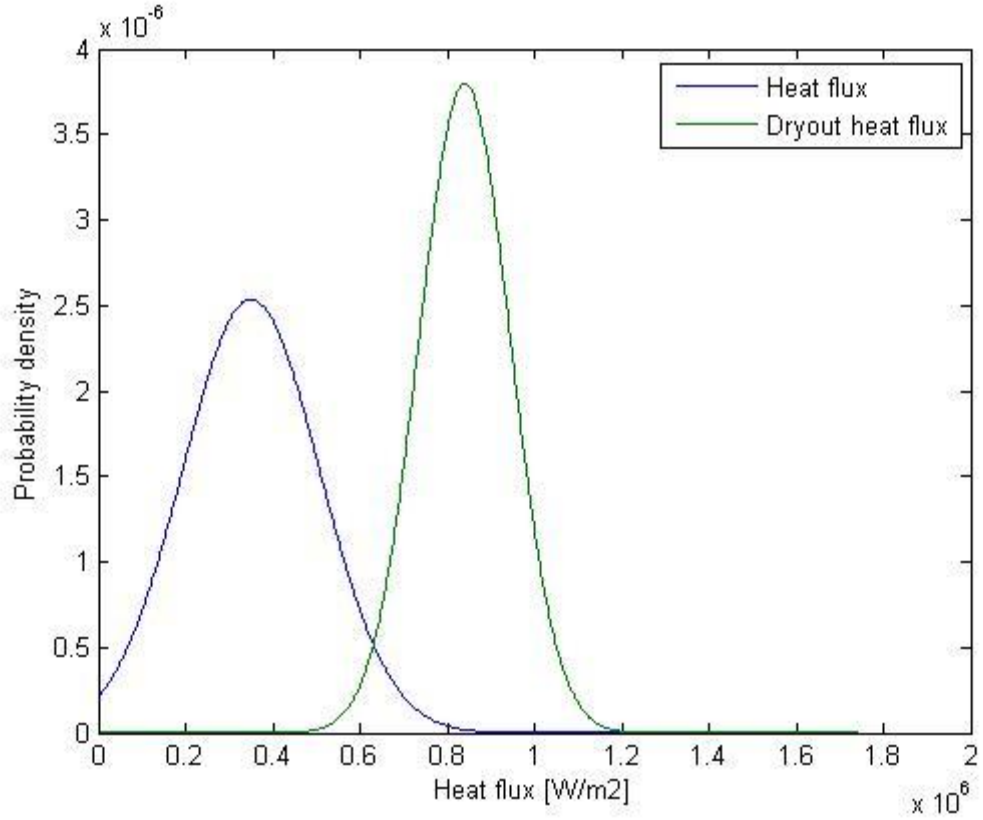

Figure 4.7: Probability density functions for heat flux and dryout heat flux in high pressure case.

Table 4.5: Probabilities of having a non-coolable debris bed in depressurized and pressurized cases calculated with eq. (7).

	Depressurized case	Pressurized case
Probability of a non-coolable debris	0.090	0.005

Although results may suggest that pressurized melt ejections could be even desirable in sense of managing severe accidents, this is of course not the case. First of all, RPV failure should be avoided at almost any cost, and by depressurizing primary system low-pressure spray can be used to provide core cooling. Pressurized vessel failure mode is also less predictable and ex-vessel steam explosions are often regarded more likely in high pressure cases. The analyses in this study may also overstate the effect of high local heat fluxes associated with heap-like debris bed configurations and ignore the improved water in-flow through the sides of the heap. Results are very sensitive to parameters used to determine probability distributions and parameter ranges and distribution shapes should be paid more attention to.

5. Conclusions

This study aimed at improving understanding of coolability of ex-vessel debris bed and its treatment in safety analyses in a risk-informed manner. Phenomenology and physics of debris coolability needs to be quite thoroughly understood, and therefore also influence of different debris bed properties and parameters as well as mechanisms through which cooling is

attained have been discussed. An important part of this study was a review of experimental work on the topic performed both at VTT and elsewhere. Especially results from another SAFIR project COOLOCE were taken a closer look at. Also analytical capabilities for ex-vessel debris bed treatment were briefly covered.

The main part of this study focused on formulating a risk-informed approach to deal with corium coolability. IDPSA methodology was utilized, which in practise meant the exploitation of MELCOR simulations. Probability of coolability was estimated with load vs. capacity concept, i.e. probability distributions were assigned to debris bed heat flux (load variable) and dryout heat flux (capacity variable). Two scenarios were considered: depressurized and pressurized melt ejection modes. Results suggested that pressurized case produces coolable debris with much higher probability, mainly because of less threatening debris bed configuration and elevated ambient pressure. However, this conclusion should of course not be taken as a guideline for severe accident management (whether to depressurize primary system or not) because accident progression in its whole complexity necessitates many other things to be taken into account as well. Nonetheless, many new insights into problems involved in ex-vessel phenomenology of a severe accident were achieved.

Appendix: MATLAB scripts

Script that samples distribution functions for load vs. capacity concept (with high system pressure) and draws plots:

```
clear all

for i=1:10000
    % Common params
    rho=7500+rand*500;     % Corium density
    M0=200*1000;           % Total corium mass
    t=3600*24*365*2*rand; % Time since reactor start-up
    Q=2.5*10^9;            % Nominal thermal power

    % Low pressure
%     eps=0.3+rand*0.1;        % Bed porosity
%     alpha=rand*25*pi/180;    % Bed angle
%     M=(100+rand*100)*1000;   % Corium mass
%     tmr=10000+rand*10000;    % Time of melt release since scram

    % high pressure
    eps=0.2+rand*0.1;        % Bed porosity
    alpha=rand*15*pi/180;    % Bed angle
    M=(150+rand*50)*1000;    % Corium mass
    tmr=15000+rand*10000;    % Time of melt release since scram

    % Debris bed height
    h=(3*M*tan(alpha)^2/(pi*rho*(1-eps)))^(1/3);
    % Specific decay heat power
    W=Q/M0*decay(t,tmr);
    % Heat flux
    HF(i)=rho*(1-eps)*W*h;
end

% Distribution functions for heat flux and dhf
x=0:2000:2*10^6-1;
% fitted pdf for heat flux
pd1=fitdist(HF','normal');
heatflux=pdf(pd1,x);
% pdf for dryout heat flux
% low pressure parameters
mu=0.8e6;
sigma=0.1e6;
% high pressure parameters
coeff=1.05;
mu=coeff*mu;
sigma=coeff*sigma;

pd2=makedist('Normal','mu',mu,'sigma',sigma);
dhf=pdf(pd2,x);
%pdf plot
plot(x,heatflux,x,dhf)
xlabel('Heat flux [W/m2]');
ylabel('Probability density');
legend('Heat flux','Dryout heat flux');
```

Function decay.m that gives relative dacay power:

```
% Decay power relative to nominal power at time of melt release
since
% start-up (t). tmr is time of melt release since reactor scram
function Prel=decay(t,tmr)
if t<tmr
    t=tmr;
end
ts=t-tmr; % time of scram
if tmr<10
    a=12.05;
    b=0.0639;
elseif tmr<150
    a=15.31;
    b=0.1807;
else
    a=27.43;
    b=0.2962;
end
Prel=5*10^-3*a*(tmr^-b-(ts+tmr)^-b);
```

References

[1] T. Silvonen, "Steam explosion case study using IDPSA methodology, Research report VTT-R-05974-13," Espoo, 2013.

[2] H.-J. Allelein and M. Bürger, "Considerations on ex-vessel corium behavior: Scenarios, MCCI and coolability," *Nuclear Engineering and Design,* vol. 236, pp. 2220-2236, 2006.

[3] S. Rahman, "Coolability of Corium Debris under Severe Accident Conditions in Light Water Reactors, Doctoral Thesis," IKE Institut für Kernenergetik und Energiesysteme (IKE), University of Stuttgart, Stuttgart, 2013.

[4] B. R. Sehgal (Ed.), Nuclear safety in light water reactors - Severe accident phenomenology, 1st ed., Elsevier, 2012.

[5] C. Journeau and H. Alsmeyer, "Validation of the COMET bottom-flooding core-catcher with prototypic corium," in *Proceedings of the ICAPP '06*, Reno, NV USA, 2006.

[6] W. Schmidt, "Influence of multidimensionality and interfacial friction on the coolability of fragmented corium," Institut für Kernenergetik und Energiesysteme (IKE), University of Stuttgart, Stuttgart, 2004.

[7] I. Lindholm, S. Holmström, J. Miettinen, V. Lestinen, J. Hyvärinen, P. Pankakoski and H. Sjövall, "Dryout heat flux experiments with deep heterogeneous particle bed," *Nuclear Engineering and Design,* vol. 236, pp. 2060-2074, 2006.

[8] M. Bürger, M. Buck, G. Pohlner, S. Rahman, R. Kulenovic, F. Fichot, W. M. Ma, J. Miettinen, I. Lindholm and K. Atkhen, "Coolability of Particulate or Porous Debris in Severe Accidents: Status and Remaining Uncertainties for In- and Ex-Vessel Scenarios," in *The 3rd European Review Meeting on Severe Accident Research (ERMSAR-2008)*, Nesseber, Bulgaria, 2008.

[9] K. Hu and T. G. Theofanus, “Scale effects and structure of dryout zone in debris bed coolability experiments,” in *Proceedings of The Sixth Meeting on Debris Coolability, Los Angeles, California, November 7–9, 1984. EPRI NP-4455*, Palo Alto, California, 1986.

[10] G. F. Stevens , "Experimental studies of dryout during boiling in particle beds at AEE Winfrith (UKAEA)," in *Proceedings of The Sixth Meeting On Debris Coolability, Los Angeles, California, November 7–9, 1984, EPRI NP-4455*, Palo Alto, California, 1986.

[11] A. W. Reed , K. R. Boldt, E. D. Gorham-Bergeron, R. J. Lipinski and T. R. Schmidt, "DCC-1/DCC-2 Degraded Core Coolability Analysis, (NUREG/CR-4390, SAND85-1967)," US Nuclear Regulatory Committee, Washington, DC, USA, 1985.

[12] L. Barleon, K. Thomauske and K. Werle, “Extended dryout and rewetting of small-particle core debris,” in *Proceedings of The Sixth Meeting on Debris Coolability Los Angeles, California, November 7–9, 1984. EPRI NP-4455*, Palo Alto, California, 1986.

[13] É. Décossin, "Numerical investigations on particulate debris bed coolability: critical analysis of the silfide experimental project," in *Proceedings of The Ninth International Topical Meeting on Nuclear Reactor Thermal Hydraulics NURETH-9*, San Francisco, California, 1999.

[14] M. J. Konovalikhin, Z. L. Yang, M. Amjad and B. R. Sehgal, "On dryout heat flux of a particle debris bed with downcomer," in *Proceedings of The 8th International Conference on Nuclear Engineering (ICONE-8)*, Baltimore, MD, 2000.

[15] K. R. Boldt , A. W. Reed and T. R. Schmidt, “DCC-3 Degraded Core coolability: Experiment and Analysis, (NUREG/CR-4606, SAND86-1033),” US Nuclear Regulatory Commission, Washington, DC, 1986.

[16] M. J. Konovalikhin, "Investigations on melt spreading and coolability in a LWR severe accident, Doctoral Thesis," Royal Institute of Technology, Stockholm, 2001.

[17] K. Simola (Ed.), SAFIR2014 - The Finnish research programme on nuclear power plant safety 2011-2014, Espoo: VTT Technical Research Centre of Finland, 2013.

[18] E. Takasuo, "Debris coolability simulations with different particle materials and comparisons to COOLOCE experiments, VTT-R-00257-13," VTT Technical Research Centre of Finland, Espoo, 2013.

[19] ASAMPSA 2, “Best-practices guidelines for L2PSA development and applications, Volume 2, Technical report ASAMPSA2/WP2-3/D3.3/2013-35,” 2013.

[20] S. E. Yakush, N. T. Lubchenko ja P. Kudinov, ”Risk-informed approach to debris bed coolability issue,” tekijä: *Proceedings of the 20th International Conference on Nuclear Engineering ICONE20*, Anaheim, CA, USA, 2012.

[21] S. Glasstone ja A. Sesonke, Nuclear Reactor Engineering, 3rd edition, London: Van Nostrand, 1981.

[22] S. E. Yakush, N. T. Lubchenko ja P. Kudinov , ”Surrogate models for debris bed dryout,” tekijä: *The 15th International Topical Meeting on Nuclear Reactor Thermal - Hydraulics, NURETH-15*, Pisa, Italy, 2013.

[23] S. E. Yakush, P. Kudinov ja N. T. Lubchenko, ”Risk and uncertainty quantification in debris bed coolability,” tekijä: *The 15th International Topical Meeting on Nuclear Reactor Thermal - Hydraulics, NURETH-15*, Pisa, Italy, 2013.

[24] Sandia National Laboratories, ”MELCOR Computer Code Manuals, Vol. 1, Primer and User's Guide, Version 1.8.6,” 2005.

[25] Sandia National Laboratories, ”MELCOR Computer Code Manuals, Vol. 2: Reference Manuals, Version 1.8.6,” 2005.

[26] I. Lindholm, ”A Review of Dryout Heat Fluxes and Coolability of Particle Beds, SKI Report 02:17,” Swedish Nuclear Power Inspectorate (SKI), 2002.

[27] T. N. Dinh, W. M. Ma, A. Karbojian, P. Kudinov , C. Tran ja C. R. Hansson, ”Ex-Vessel Corium Coolability and Steam Explosion Energetics in Nordic Light Water Reactors, Research report NKS-160,” Nordic nuclear safety research NKS, Roskilde, 2008.

[28] "Wikipedia - Sparging (chemistry)," [Online]. Available: http://en.wikipedia.org/wiki/Sparging_(chemistry). [Accessed 21st May 2014].